New Phytologist

Research

The genetic architecture of petal number in *Cardamine hirsuta*

Bjorn Pieper, Marie Monniaux and Angela Hay

Max Planck Institute for Plant Breeding Research, Carl-von-Linné-Weg 10, 50829 Köln, Germany

Author for correspondence:
Angela Hay
Tel: +49 221 5062108
Email: hay@mpipz.mpg.de

Received: *20 April 2015*
Accepted: *4 July 2015*

New Phytologist (2016) **209:** 395–406
doi: 10.1111/nph.13586

Key words: *Cardamine hirsuta*, comparative development, natural variation, petal number, quantitative trait locus (QTL).

Summary

- Invariant petal number is a characteristic of most flowers and is generally robust to genetic and environmental variation. We took advantage of the natural variation found in *Cardamine hirsuta* petal number to investigate the genetic basis of this trait in a case where robustness was lost during evolution.
- We used quantitative trait locus (QTL) analysis to characterize the genetic architecture of petal number.
- Average petal number showed transgressive variation from zero to four petals in five *C. hirsuta* mapping populations, and this variation was highly heritable. We detected 15 QTL at which allelic variation affected petal number. The effects of these QTL were relatively small in comparison with alleles induced by mutagenesis, suggesting that natural selection may act to maintain petal number within its variable range below four. Petal number showed a temporal trend during plant ageing, as did sepal trichome number, and multi-trait QTL analysis revealed that these age-dependent traits share a common genetic basis.
- Our results demonstrate that petal number is determined by many genes of small effect, some of which are age-dependent, and suggests a mechanism of trait evolution via the release of cryptic variation.

Introduction

Stable merosity (the number of organs within whorls) is one of the major trends in angiosperm floral evolution (Specht & Bartlett, 2009). The majority of core eudicots and monocots have fixed pentamerous and trimerous merosity, respectively, while members of the Brassicaceae are characterized by a fixed cruciform arrangement of four petals. This cruciform flower is typified by the model species *Arabidopsis thaliana*, which contains four petals, surrounded by four sepals, and internal to these sterile organs are the reproductive organs: stamens and carpels. *Cardamine hirsuta* is related to *A. thaliana* and shares a similar four-whorled flower but petal number is unstable, varying from zero to four between individual flowers.

The precise identity, number and placement of floral organs is defined early in flower development and is under strict genetic control (Coen & Meyerowitz, 1991). However, while the genetic basis of floral organ identity is well understood and encapsulated in the predictive ABC model (Bowman *et al.*, 1991), we know less about the genes that control the specific number of different floral organs. The production of four petals in *A. thaliana* requires genes that control petal identity and the establishment of boundaries that demarcate the position of petal initiation on the floral meristem (Irish, 2008; Huang *et al.*, 2012; Lampugnani *et al.*, 2013). However, this gene activity must also interface with pathways that control the size of the floral meristem, the outgrowth of lateral organs and the patterning of their polarity, and these interactions are not yet captured by predictive models (Eshed *et al.*, 2001; Benkova *et al.*, 2003; Irish, 2008). Two important gene products for petal organogenesis are the trihelix transcription factor encoded by *PETAL LOSS* (*PTL*) and the zinc-finger transcriptional repressor encoded by *RABBIT EARS* (*RBE*) (Brewer *et al.*, 2004; Takeda *et al.*, 2004). Mutations in these genes cause a reduction in petal number, which is associated with a failure to suppress the growth in the boundary region between sepals (Brewer *et al.*, 2004; Krizek *et al.*, 2006; Lampugnani *et al.*, 2012). RBE promotes activity of the microRNA-regulated *CUP-SHAPED COTYLEDON1/2* (*CUC1/2*) boundary genes by direct repression of *MIR164c*, while *PTL* acts in parallel to *CUC1/2* to suppress growth between sepals, and this boundary delimitation is required for auxin-induced petal initiation (Huang *et al.*, 2012; Lampugnani *et al.*, 2013).

The analysis of natural genetic variation offers additional insights over induced mutants about which components of a gene regulatory network were targeted by evolution to generate diversity. Natural variation in *A. thaliana* has proved an important resource to dissect the genetic basis of developmental traits (Michaels & Amasino, 1999; Johanson *et al.*, 2000), however, petal number does not vary among *A. thaliana* accessions. This reproducibility of petal number reflects its robustness to genetic variation. Phenotypic robustness is a property of many developmental patterning systems but is challenging to address experimentally. Studies in *Caenorhabditis* show that vulva cell fate patterning is invariant but evolves by accumulating cryptic variation (Felix, 2007; Milloz *et al.*, 2008). In *C. hirsuta*, the normally invariant trait of petal number expresses phenotypic variation,

providing an opportunity to analyse quantitative genetic variation that may be cryptic in species with robust petal number such as *A. thaliana*. Moreover, this comparative system of two related, genetically tractable species that differ in phenotypic robustness, provides an opportunity to functionally address the contribution of cryptic variation to trait evolution.

Fisher's polygenic model of inheritance attributes the genetic architecture of quantitative traits to a small number of variants with large effects and a large number of variants with small effects (Fisher, 1918). Major quantitative trait locus (QTL) have been identified in both plants and animals that produce large morphological effects (Doebley *et al.*, 1997; Shapiro *et al.*, 2004; Johnston *et al.*, 2013). But on the other hand, studies of quantitative traits in humans have found the largest QTL effect sizes to be small; and much of the variation in these studies remains unmapped, contributing to the notion of missing heritability (Manolio *et al.*, 2009). Therefore, it may be difficult to generalize about the number and effect size of alleles that underlie any quantitative trait, as attributes of both the species and the trait being studied will influence the type of genetic variation found (Stern & Orgogozo, 2008; Rockman, 2012). For these reasons, describing the genetic architecture of petal number variation in *C. hirsuta* addresses both general and particular questions of trait evolution.

In this work, we identify QTL controlling mean petal number in five mapping populations derived from bi-parental crosses between diverse *C. hirsuta* accessions. We further characterize phenotypic variation around the mean petal number in these populations and show that this variation is not stochastic but age-dependent. We use multi-trait QTL analysis to show that petal number shares a common genetic basis with another age-dependent trait, sepal trichome number. We investigate the age-dependent genetic control of petal number and sepal trichome number in *C. hirsuta* by detecting QTL effects during discrete intervals of developmental time, and recover the same loci that affect average petal number plus additional loci with age-specific effects. Our results indicate that petal number is a complex trait controlled by many QTL of small to moderate effect, some of which are involved in general or trait-specific responses to ageing.

Materials and Methods

Genetic material

Five independent *C. hirsuta* L. mapping populations were analysed that had the Oxford (Ox) accession as a recurrent parent (specimen voucher Hay 1 (OXF); Hay & Tsiantis, 2006). The Ox × Wa F_8 recombinant inbred line (RIL) population is described in Hay *et al.* (2014). The Ox × Az RIL population consisted of 150 F_7 lines derived from a cross between Ox and an accession collected from the Azores islands (gift from M. Tsiantis). The Ox × GR RIL population (Cartolano *et al.*, 2015) consisted of 192 F_7 lines (189 lines genotyped for mapping; phenotype of 179 used for QTL analysis) derived from a cross between Ox and the accession GR, collected in Athens, Greece (Hay *et al.*, 2014) (gift from M. Tsiantis). The Ox × Nz F_2 population consisted of 297 plants derived from a cross between Ox and the Nz accession collected from Wellington, New Zealand (Hay *et al.*, 2014). The Ox × Jpa1 F_2 population consisted of 418 plants, derived from a cross between Ox and the Jpa1 accession collected from Oumi, Japan (Hay *et al.*, 2014), of which 100 lines belonging to both extremes of the phenotypic distribution were selected for genetic analysis.

EMS mutagenesis

C. hirsuta Ox seeds were mutagenized by agitation with 0.2% ethane methanesulfonate (EMS, Sigma) for 10 h, washed in dH_2O, then sown on soil and harvested in pools of five M1 plants. Approximately 1500 M2 plants were subsequently screened to identify the *fp2* mutant. Mutant characterization was performed after backcrossing to Ox twice.

Genetic map

The genetic map for the Ox × Wa RILs is described in Hay *et al.* (2014). For the Ox × GR, Ox × Jpa1 and Ox × Nz populations, only partial genomic coverage could be achieved by genotyping with available markers from the Ox × Wa genetic map. The total coverage of linkage groups was 39.4%, 58.0% and 26.3% for those populations, respectively, when compared with the Ox × Wa map (Hay *et al.*, 2014). Furthermore, 7, 2 and 6 loci were represented by independent markers in these three populations, respectively. Therefore, an integrated genetic map was made from the five individual maps for QTL analysis that consisted of 345 markers and had a total length of 891.7 cM (Supporting Information Fig. S1). All genetic maps were made using the regression mapping algorithm of Joinmap® 4 (Van Ooijen, 2006).

Plant cultivation

Plants were grown 7 × 7 cm pots on a 3 : 1 peat–vermiculite mixture. All experiments were performed under a photoperiod of 16 h : 8 h, light : dark. Experiments with the Ox × Wa and Ox × GR RILs, and the Ox × Jpa1 F_2 were conducted in a glasshouse with supplemental light and a temperature of 20°C. The Ox × Az RIL population was analysed in a controlled environment chamber with temperatures of 19°C : 18°C, day : night. The Ox × Nz F_2 population was analysed in a controlled environment chamber with temperatures of 22°C : 21°C, day : night. The *fp2* mutant and Ox were grown in a controlled environment chamber with constant temperature of 23°C to analyse petal number and in a glasshouse with supplemental light and a temperature of 20°C to analyse other phenotypes.

Plant phenotyping

Up to 30 of the first flowers to develop on the main inflorescence were consecutively removed from the plant as they opened and the petal number and the total number of trichomes present on the sepals were counted using a dissecting microscope. For the

Ox × Wa and Ox × Az populations, three replicate lines were analysed per RIL, while for the Ox × GR population a single line was analysed. The average number of petals and sepal trichomes were calculated per plant and used for QTL analysis in the F2 populations and in the Ox × GR RIL population, while for the other populations the mean average per RIL was used. Petal number in *fp2* and Ox was scored in up to 15 of the first flowers of 12 plants ($n = 171$) and 15 plants ($n = 225$), respectively. Other floral organs in *fp2* and Ox were scored in up to 25 of the first flowers of nine plants ($n = 193$) and seven plants ($n = 159$), respectively. Rosette leaf number and the average leaflet number in *fp2* and Ox were scored in nine and seven plants, respectively. Rosette leaf number was scored as the number of rosette leaves initiated when the first floral buds were visible; leaflet number was scored on all leaves.

Quantitative trait locus analysis

All statistical analyses, including QTL analysis, were done using GenStat 16th edition (VSN International, 2013). Broad sense heritabilities (H^2) were calculated according to the implementation in GenStat: 1 – ((non-genetic (within RIL) variance/number of plants per RIL)/genetic (between RILs) variance component), where the variance components are estimated by fitting a mixed model with RIL as a random term. For QTL analysis, genetic predictors were calculated from the molecular marker data and the integrated genetic map with a maximum distance of 2 cM between them. The QTL mapping methodology for multi-trait QTL analysis involved fitting a mixed effects model to a set of traits in which the QTL were fixed effects and the residual genetic and non-genetic variances and covariances were modelled by a random term. The method for single trait analysis is similar but in this case only the residual genetic and nongenetic variance was modelled by the random term. Simple interval mapping scans were followed by several iterations of composite interval mapping. During the latter procedure, cofactors were added and/or removed until no further improvement could be made. The genetic predictors comprising the final set of co-factors were used for fitting the final QTL models in GenStat to estimate the additive allelic effects. The total phenotypic variances explained by the full QTL models were determined as the difference in the residual variance components of the models with no QTL vs the models with all QTL fitted. These differences were then expressed as the percentages of the residual variances from the models with no QTL fitted. In Tables 1 and 2, the phenotypic variances explained by each QTL were estimated as the differences in the total variance explained by the full QTL model and models where each QTL was successively dropped. In SI Tables, we used the QMTESTIMATE procedure in GenStat to estimate the variance explained per QTL. The average number of petals or sepal trichomes per flower were calculated per plant and used for single trait QTL analysis in the F_2 populations and in the Ox × GR RILs, while for the other populations the mean average per line was used. Multi-trait QTL analysis was performed on the average petal number and average sepal trichome number, as well as on the averages per bin of five flowers. For the latter procedure, the respective phenotypic data were averaged per five flowers, without overlap, for up to as many as 30 flowers, thus yielding six averages per trait per plant. A multi-trait genome scan was then performed using the set of 12 averages as traits. Following this analysis, moving averages were calculated for each trait per plant per three flowers, with increments of one flower (except for the first of the averages which was an average of only flowers 1 and 2), thus yielding up to 29 trait averages across the flowering shoot. A final multi-trait QTL model with the QTL detected for the nonoverlapping five flower bins was then fitted to the 29 petal and sepal trichome moving averages. Estimating the QTL effects in this way allowed us to determine how they changed over time.

Statistical analysis

In order to determine whether flower rank and genotype were independent predictors of the petal number of individual flowers in the mapping populations, petal number was modelled as a function of the fixed terms genotype and flower rank. The model was fitted using the REML directive of GenStat and the significance of the fixed terms was evaluated by the associated Wald tests. The variance explained by flower rank was determined as the difference between the residual variance components of models with (1) only genotype and (2) both genotype and flower rank fitted, as a percentage of the residual variance component of a model with neither of the terms fitted.

Table 1 Characteristics of quantitative trait loci (QTL) detected for average petal number in five *Cardamine hirsuta* mapping populations

QTL	Population	Linkage group	Position (cM)	Add. eff. (petals)	Var. expl. (%)
PN1	Ox × Az	Chr.1	45.88	−0.39	4.4
PN2	Ox × Wa	Chr.2	6.85	−0.75	13.2
	Ox × GR	Chr.2	6.85	−0.44	4.4
PN3	Ox × Az	Chr.3	15.29	0.47	5.2
PN4	Ox × Az	Chr.4	39.92	0.63	10.1
	Ox × Jpa1	Chr.4	39.92	2.12	13.5
PN5	Ox × Az	Chr.4	80.26	−0.53	7.8
	Ox × GR	Chr.4	81.98	0.49	4.7
PN6	Ox × Wa	Chr.4	93.89	0.54	6.2
	Ox × Nz	Chr.4	95.99	0.37	3.6
PN7	Ox × Wa	Chr.5	11.15	−0.44	4.4
PN8	Ox × Jpa1	Chr.5	57.49	−1.80	11.9
	Ox × Wa	Chr.5	67.22	−0.51	5.9
PN9	Ox × Nz	Chr.6	68.24	0.55	7.9
	Ox × GR	Chr.6	72.56	0.46	4.3
PN10	Ox × Az	Chr.6	100.05	−0.44	5.6
PN11	Ox × Nz	Chr.6	112.39	−0.91	13.9
PN12	Ox × Az	Chr.7	36.57	−0.44	4.6
PN13	Ox × GR	Chr.7	116.62	0.53	6.8
PN14	Ox × Wa	Chr.8	0.00	0.92	21.8
	Ox × Az	Chr.8	1.04	0.65	14.0
	Ox × Jpa1	Chr.8	8.42	1.84	10.0
PN15	Ox × GR	Chr.8	69.37	−0.54	6.5

Additive effects (Add. eff.) are given for homozygous allele substitutions with Ox alleles. Var. expl., phenotypic variance explained by the QTL.

Table 2 Characteristics of the multi-trait quantitative trait loci (QTL) detected for average petal number and average sepal trichome number in two *Cardamine hirsuta* mapping populations

				Average petal number		Average sepal trichome number	
QTL	Pop	LG	Position (cM)	Add. eff. (petals)	Var. expl. (%)	Add. eff. (trichomes)	Var. expl. (%)
P-T1	Ox × Az	Chr.1	44.83	−0.55	6.0	−0.38	2.9
[1]	Ox × Az	Chr.2	29.16	−0.49	4.8	0.25	1.1
P-T4	Ox × Az	Chr.3	10.51	0.49	4.0	0.43	3.2
P-T5	Ox × Az	Chr.4	39.92	0.66	7.6	ns	ns
P-T6	Ox × Az	Chr.4	81.98	−0.61	6.6	ns	ns
P-T7	Ox × Nz	Chr.4	93.89	0.34	2.3	−0.58	6.8
P-T8	Ox × Az	Chr.5	20.05	ns	ns	0.55	5.1
P-T9	Ox × Az	Chr.5	57.49	ns	ns	0.61	4.3
P-T10	Ox × Nz	Chr.6	68.24	0.57	8.2	ns	ns
P-T11	Ox × Az	Chr.6	94.35	−0.60	7.3	0.43	3.8
P-T12	Ox × Nz	Chr.6	110.83	−0.90	13.4	ns	ns
P-T13	Ox × Az	Chr.7	8.46	ns	ns	−1.07	20.4
P-T14	Ox × Nz	Chr.7	47.58	ns	ns	0.48	4.6
P-T15	Ox × Az	Chr.7	79.71	ns	ns	−0.65	5.9
P-T16	Ox × Nz	Chr.7	99.37	0.31	1.3	−0.62	4.3
P-T17	Ox × Az	Chr.8	1.04	0.72	11.2	−0.42	3.7
[1]	Ox × Az	Chr.8	55.29	ns	ns	0.70	9.3

pop, population in which the respective QTL was detected; LG, linkage group. The positions where the detected QTL effects were most significant are shown in centi-Morgan. Additive effects (Add. eff.) are given as a change in either petal number or sepal trichome number for homozygous allele substitutions with Ox alleles. Var. expl., percentage of phenotypic variance explained by the QTL. ns, nonsignificant effects. [1]QTL are named according to the analysis summarized in Fig. 4(e) and Supporting Information Table S2 but as a consequence the two QTL indicated have no equivalent named locus.

Results

To elucidate the genetic architecture of petal number variation, we analysed five independent mapping populations generated from bi-parental crosses with the Ox accession as a recurrent parent. Average petal number in these experimental populations covered a range from 0 to 4, however, flowers with more than four petals were never observed. Transgressive variation was observed in all populations, leading to average petal numbers that exceeded those of the founder accessions, and the broad sense heritability (H^2) of this variation was high (0.86–0.90), demonstrating a strong genetic basis for this trait (Fig. 1). We found that petal number varied in response to slight differences in the environmental conditions between separate experiments, suggesting that this trait is determined not only by genetics but also by environment. These effects are most prominent when comparing the average petal number of the recurrent parent Ox between different experiments (Fig. 1). The extensive transgression in these mapping populations indicates that average petal number differences between the founder accessions are not consistent with directional natural selection (Orr, 1998). Furthermore, it shows that there is sufficient standing variation in our sample to generate petal numbers across the possible range of 0–4 through recombination.

Quantitative trait locus analysis of average petal number was performed in order to discover the loci at which allelic variation affected this trait and to estimate their effects. We detected 15 distinct QTL in total at which allelic variation affected petal number when considering loci identical if < 10 cM apart (Figs 2, S2, Table 1). Despite partial genomic coverage of some genetic maps, three QTL were detected in the Ox × Nz and Ox × Jpa1 populations, seven QTL in the Ox × Az population and five QTL in each of the other populations. With the exception of the

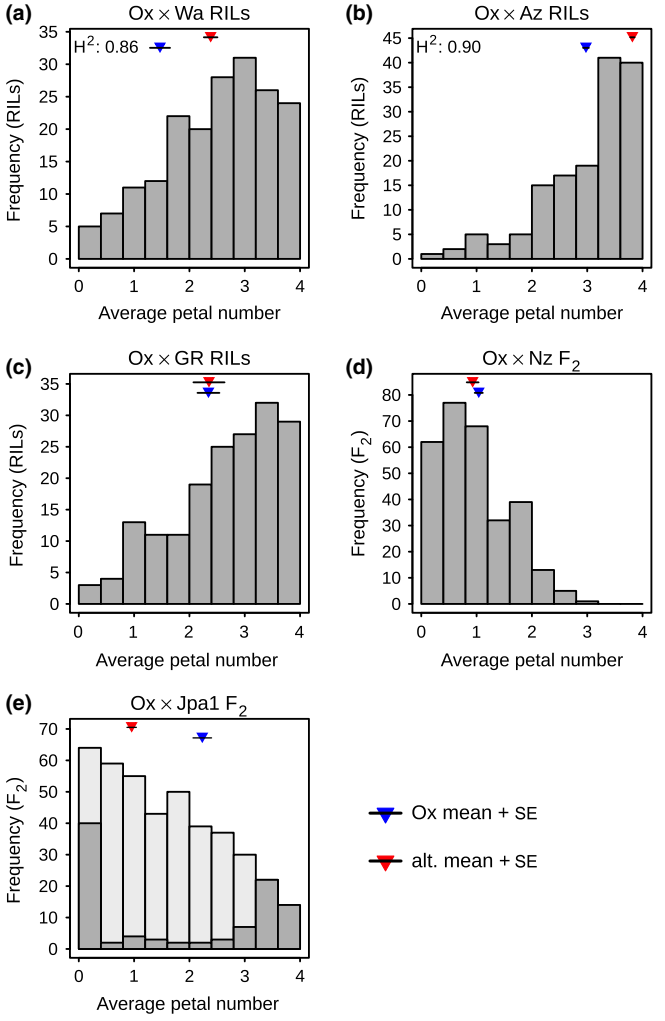

Fig. 1 Distribution of average petal number in five experimental populations of *Cardamine hirsuta*. Frequency histograms showing the distributions of average petal number in the following populations: (a) Ox × Wa recombinant inbred lines (RILs), (b) Ox × Az RILs, (c) Ox × GR RILs, (d) Ox × Nz F_2, and (e) Ox × Jpa1 F_2; data shown for the complete population (light plus dark grey) and lines selected from the tails of the distribution for genetic analysis (dark grey). Mean petal number of the Ox parent (blue triangle) and the alternative parent (red triangle) are indicated. Horizontal lines through the triangles indicate the standard errors of the means. Broad sense heritability (H^2) of the variation in petal number is included in the upper left corner in (a, b) (note that H^2 was not estimated in c–e because replicates of genetically identical plants were not available for these populations).

Ox × Jpa1 population, at least one unique QTL for petal number was always detected. The full additive QTL models explained up to 56.2% (for the Ox × Wa RILs; Table S1) of the total phenotypic variance for average petal number.

To further investigate the genetic architecture of petal number, we examined the allelic effects of the detected QTL. Both negative and positive allelic effects on petal number were found in all mapping populations, which is consistent with the observed transgressive variation. The strongest effects were observed in the Ox × Jpa1 F_2 population with the largest effect being 2.12 petals for QTL *PN4* (Table 1). However, selection of plants from the extremes of the phenotypic distribution has likely led to an overestimation of these effects (see the Materials and Methods section). *PN4* was also detected in the Ox × Az RIL population with an allelic effect of 0.63 petals, and another two QTL detected in the Ox × Jpa1 F_2, *PN8* and *PN14*, also had considerably weaker effects in the other populations where these were detected. The strongest effects observed in the unbiased populations was 0.92 and −0.91 petals for homozygous substitutions with Ox alleles in the Ox × Wa RIL population at *PN14* and the Ox × Nz F_2 population at *PN11* respectively. The absolute magnitude of all other QTL effects ranged between 0.37 and 0.75 petals for homozygous substitutions. We found that mutant alleles induced by ethyl methanesulfonate (EMS) in the Ox accession can have much stronger effects on petal number than the natural alleles detected in our mapping populations. For example, a recessive allele of the *four petals 2* (*fp2*) mutant increased the average petal number by 2.0 over the wild-type value when homozygous (Fig. 3a,b). We observed no pleiotropic effects of the *fp2* mutant on the number of other floral organs, the number of rosette leaves produced before flowering, or the number of leaflets per leaf, suggesting that *fp2* specifically affects petal number (Fig. 3c–e). This result shows that single mutations can produce large phenotypic effects on petal number but such large-effect alleles are not found in natural accessions of *C. hirsuta*.

To understand petal number in the context of variation found in other floral organs in *C. hirsuta*, we compared the location of QTL identified here with those previously identified for stamen

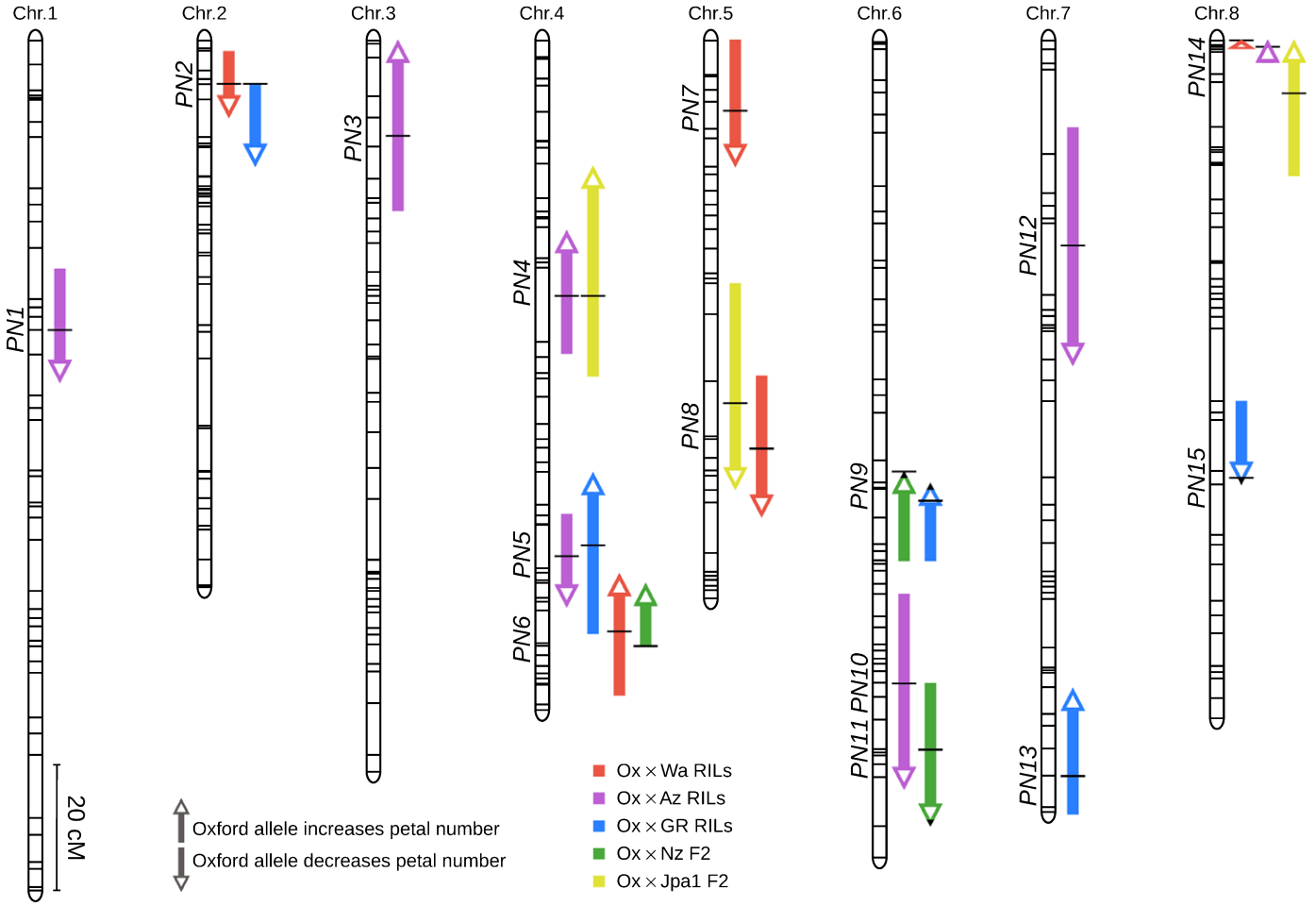

Fig. 2 Genetic architecture of petal number in *Cardamine hirsuta*. Quantitiative trait loci (QTL) for average petal number detected in five mapping populations are shown as arrows on the eight linkage groups of the integrated genetic map. Positions with the most significant effects are indicated by horizontal black lines and the length of the arrows is scaled to the 2-log(p) interval for each QTL. Arrows are terminated with a black mark where the most probable position of the QTL or the 2-log(p) interval could not be accurately determined due to incomplete map coverage. Arrows point up or down according to whether the Ox allele increases or decreases petal number. Different colours indicate the population in which the QTL was detected. QTL are numbered *PN1* through *PN15* and shown to the left of the linkage groups.

number in the Ox × Wa RILs (Hay *et al.*, 2014). We found that the major QTL influencing petal and stamen number did not co-locate, indicating that each trait has a distinct genetic basis. We next considered how petal number varied within individual plants. Following the phase transition from vegetative to reproductive development in *C. hirsuta*, the shoot apical meristem remains indeterminate, yet produces floral meristems on its flank rather than leaf primordia. Modelling petal numbers on individual flowers as a function of genotype and flower rank (i.e. the number in sequence when counting from the first flower to develop) revealed that the rank of the flower was a highly significant source of variation ($P < 0.001$). Although most variance for petal number per flower was explained by genotype in the populations, up to 16% of the remaining variance was accounted for by flower rank. This observation indicated that the variance around the mean petal number per plant was not random but rather, there existed a strong relationship between the rank of the flower and the number of petals it produced. Closer inspection revealed a typical pattern whereby petal number on the first flowers to open was relatively high, and would then decrease over time, to eventually rise again towards the last flowers that a plant produced (Fig. 4a). To gain insight into this temporal pattern, we sought to identify another quantitative floral trait that is temporally regulated to compare its dynamics with that of petal number. Trichome distribution is a classical marker of developmental phase transitions in *A. thaliana* (Telfer *et al.*, 1997). The distribution of trichomes during flowering is temporally regulated by microRNA156-targeted *SQUAMOSA PROMOTER BINDING PROTEIN LIKE (SPL)* genes in *A. thaliana* (Shikata *et al.*, 2009; Yu *et al.*, 2010), which increase in expression due to a decline in miR-156 levels as the plant ages (Wang *et al.*, 2009). We quantified trichome distribution on the abaxial surface of sepals in *C. hirsuta* and found that the temporal change in sepal trichome number closely resembled that of petal number (Fig. 4a,b). Based on this observation that the two traits co-varied during plant ageing, we hypothesized that they may share a common genetic basis.

To investigate whether the genetic basis of petal number variation, a derived trait in *C. hirsuta*, shared common components with sepal trichome density; a conserved trait between *C. hirsuta* and *A. thaliana*, we performed multi-trait QTL analysis of both traits. We quantified petal number and sepal trichome number in the Ox × Nz F_2 and the Ox × Az RIL populations and observed transgression beyond the trait values of the founder accessions in both populations (Fig. 4c, d). This variation in sepal trichome number was highly heritable with an H^2 of 0.74 in the RIL population, where broad sense heritability could be determined, indicating that trichome number has a strong genetic basis. We detected 12 QTL in the Ox × Az RIL population using multi-trait QTL analysis of average petal number and trichome number, and five different QTL in the Ox × Nz F_2 population (Figs 4e, S3, Table 2). Five of the QTL detected in the Ox × Az population had significant effects on both petal number and trichome number (*P-T1*, *4*, *11*, *17* and the QTL on chromosome 2 between *P-T2* and *P-T3*) while two QTL affected only petal number (*P-T5*, *6*) and five QTL affected only trichome number

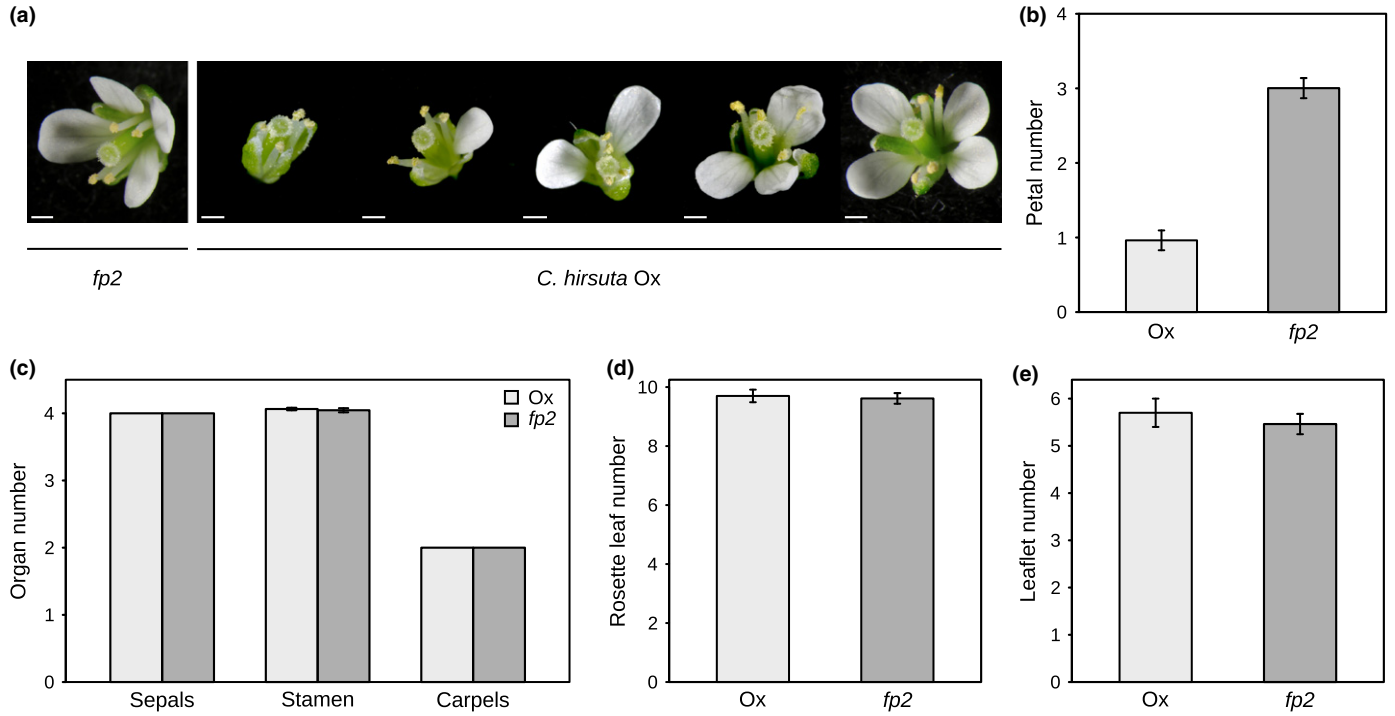

Fig. 3 The non-pleiotropic *four petals2* mutant increases petal number in *Cardamine hirsuta*. (a) Representative flower showing the model petal number found in *fp2* (left) and representative flowers of all petal numbers found in wild type Ox (right). (b) Barchart showing average petal number in wild type Ox and *fp2* genotypes grown at 23°C, $n = 225$ and 171 flowers, respectively. (c–e) Barcharts showing average floral organ numbers (c, $n = 159$ and 193 flowers, respectively), average rosette leaf number (d, $n = 7$ and 9 plants, respectively), and average leaflet number (e, $n = 7$ and 9 plants, respectively) in wild type Ox (light grey) and *fp2* (dark grey) genotypes. Error bars show ± SE of the mean.

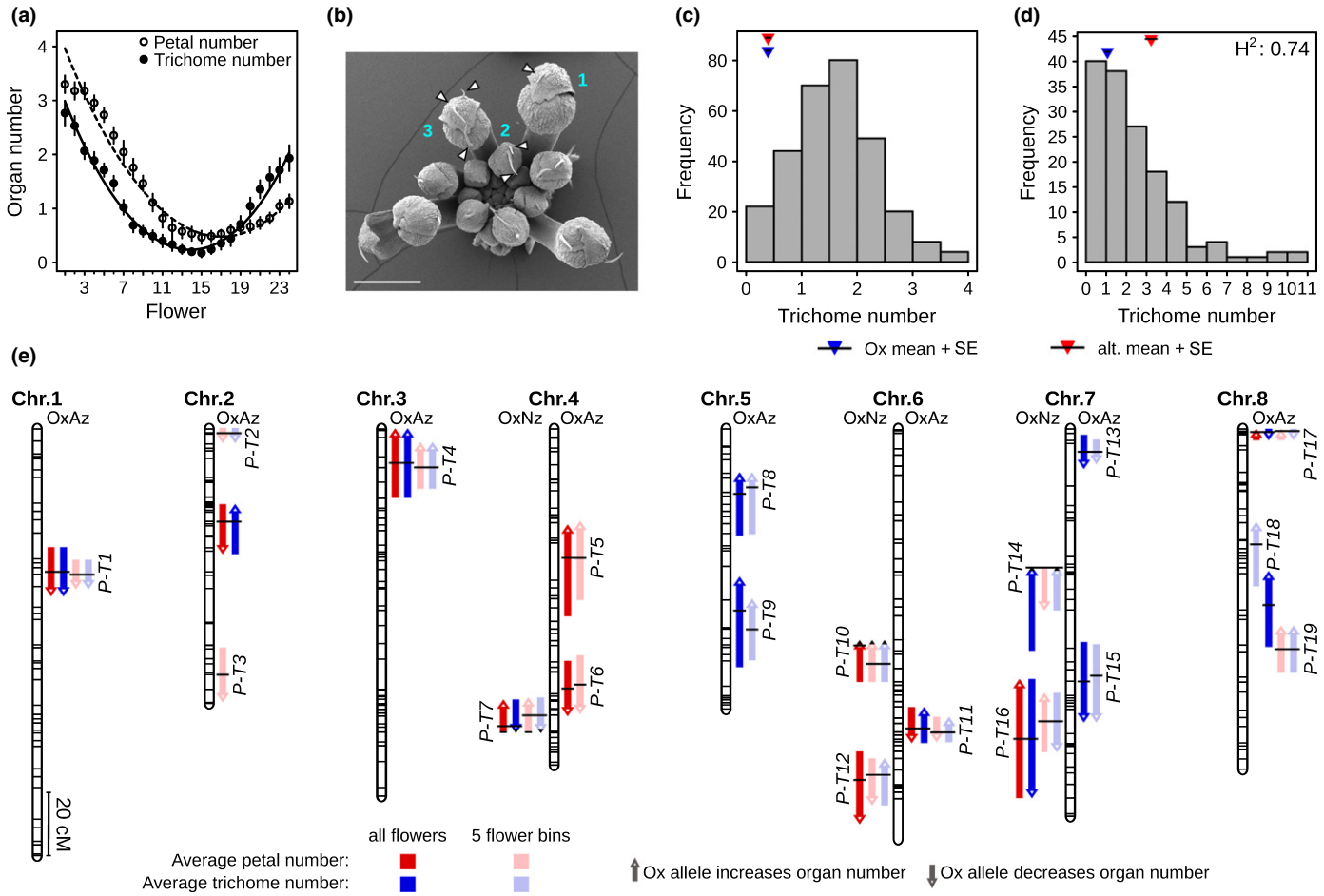

Fig. 4 Petal and sepal trichome number share a common genetic basis in *Cardamine hirsuta*. (a) Moving averages of petal number (open circles) and sepal trichome number (closed circles) show a similar age-dependent change when plotted against flower position. Organ counts were averaged in a window of three flowers that was shifted by one flower except the first average, which was calculated for flowers 1 and 2. Dashed and continuous lines show nonlinear models fitted to the petal and trichome numbers, respectively, to illustrate the similarity in their relation with flower number. (b) Scanning electron micrograph of a *C. hirsuta* inflorescence; varying numbers of sepal trichomes are indicated by arrowheads on representative flowers with 1, 2 and 3 trichomes; bar, 0.5 mm. (c, d) Frequency distributions of average sepal trichome number in the Ox × Nz F_2 (c), and the Ox × Az recombinant inbred lines (RILs) (d). Mean average sepal trichome number for the founder accessions of each population is indicated by triangles (Ox: blue, Az or Nz: red) and the standard error of the mean by the black line crossing it. (e) Summary of multi-trait quantitative trait locus (QTL) analysis of petal and sepal trichome numbers averaged over all flowers and in consecutive bins of five flowers (up to as many as 30 flowers). Detected QTL are shown as arrows on the integrated genetic map to either the left (Ox × Nz F_2) or the right (Ox × Az RILs) of the eight linkage groups according to the mapping population in which they were detected. The black marker inside each arrow is placed at the position where the detected QTL effect was most significant and the length of each arrow is scaled to a 2-log(p) interval around that position. Arrows are terminated with a black mark where the most significant position or the 2-log(p) interval could not be accurately determined due to incomplete map coverage. Arrows point up or down according to whether the Ox allele increases or decreases petal number. The two traits are shown in different colours: petal number (red) and sepal trichome number (blue), and the phenotyping method is indicated by colour shade: averaging all flowers (bright) and averaging five flower bins (pale). The number of traits analysed with multi-trait QTL analysis of the binned averages totalled to 10 and 12 for the Ox × Nz F_2 and the Ox × Az RILs, respectively. The results are summarized with a single arrow if a significant effect was detected for at least one bin. The direction was always the same when effects were detected in multiple bins.

(*P-T8*, *9*, *13*, *15* and the QTL on chromosome 8 between *P-T18* and *P-T19*). Six of the QTL with effects on petal number had been detected in our previous analysis (*PN1*, *3*, *4*, *5*, *10*, and *14*; Fig. 2; Table 1). We found that the weakest effect QTL detected in our previous analysis (*PN12*; Fig. 2; Table 1) was no longer significant but we detected a novel QTL effect on petal number on chromosome 2 at 29.16 cM, accompanied by a significant effect on trichome number (Fig. 4e between *P-T2* and *P-T3*, Table 2). We detected two QTL with effects on both petal number and trichome number in the Ox × Nz F_2 population (*P-T7*, *16*) that had both been detected before as QTL affecting petal number (*PN6*, *13*; Fig. 2, Table 1), and another three QTL had effects on only petal number (*P-T10*, *12*) or trichome number (*P-T14*). All three QTL that we had previously detected in this population (*PN6*, *9* and *11*; Fig. 2, Table 1) were also found using multi-trait QTL analysis. In summary, 7 of 11 QTL that affected petal number also had significant effects on trichome number, showing that indeed both traits are partly under the control of the same loci, either pleiotropically or due to closely linked QTL. However, these loci did not consistently affect both

traits in the same way: at five QTL (*P-T7*, *11*, *16*, *17* and the QTL on chromosome 2 between *P-T2* and *P-T3*) the allelic effects for petal number and trichome number were of opposite sign while at the remaining two QTL (*P-T1*, *4*) they were of the same sign. Therefore, averaging petal number and trichome number per plant may obscure the age-dependent effects of these alleles on each trait.

Age-dependent variation in petal and sepal trichome number appeared as uncertainty around the average trait values in our analysis above, while this may actually be under genetic control. Considering the relationship between the age of the shoot and the numbers of petals and sepal trichomes produced by flowers, and the similarity in temporal patterning of both traits, we investigated whether and how QTL affected these traits in an age-dependent manner. To do this, we performed multi-trait QTL analysis on petal number and trichome number averaged in nonoverlapping bins of five flowers (i.e. 12 averages in the Ox × Az population and 10 in the Ox × Nz population). Across both populations, 19 QTL were detected with significant effects on at least one bin for either petal number or trichome number (Figs 4e, S4, Tables S2–S4). These QTL included the same loci as we found with multi-trait analysis of petal number and trichome number averaged over the entire inflorescence, with a few exceptions. For example, a QTL was detected for petal number and trichome number averaged across all flowers in the Ox × Az population on chromosome 2 at 29.16 cM (between *P-T2* and *P-T3*), whereas a QTL for petal number and trichome number in binned flowers (*P-T2*) was detected at 1.23 cM instead (Fig. 4e, Table S2). Allelic effects of the age-dependent QTL (*P-T2*) were of the same sign for petal number and trichome number while those of the QTL for average petal number and trichome number were of the opposite sign (Fig. 4e, Table S3). In another example from the same population, two separate QTL were detected on chromosome 8 at 36.55 and 69.37 cM: one for trichome number (*P-T18*), and one for petal number and trichome number (*P-T19*), in binned flowers (Fig. 4e, Table S2), whereas a single QTL for average trichome number was found between them at 55.29 cM. These differences are probably caused by closely linked QTL in each case, which hindered the accurate determination of the QTL position on chromosome 2, while the single QTL effect on average trichome number on chromosome 8 was resolved into two distinct loci (Fig. 4e, Table S2). Interestingly, we detected 13 of the 15 QTL that we previously detected for average petal number across all five populations, as QTL for petal number and/or trichome number using only two populations (Ox × Az RIL and Ox × Nz F_2; Table S2). The increased power of multi-trait analysis and the increased accuracy of phenotyping by binning flowers rather than averaging across all flowers, resulted in the detection of significant effects on both petal number and trichome number at 11 out of the 19 QTL, lending further support to the notion that the two traits are under common genetic control. These results also showed that some QTL indeed acted in an age-dependent manner as the significance or strength of their allelic effects changed over consecutive bins (Tables S3, S4).

To accurately determine the age-dependent effects of the 19 detected QTL, we fit the final multi-trait QTL model of petal number and trichome number in binned flowers, to trait values averaged in a sliding window of three flowers to give an overlapping moving average (Fig. 5a, Tables S5, S6). This analysis revealed that the effect of different QTL could be either consistent, or increasing, or decreasing in strength and significance during ageing of the shoot (Fig. 5b–e). We found both correlated as well as anti-correlated QTL effects on petal number and trichome number but the direction of effects never changed significantly for any single QTL (Fig. 5). Those QTL that mostly affected either petal number or trichome number tended to have consistent effects during ageing of the shoot (*P-T5*, *6*, *8*, *9*, *13*, *15*, *18*). In other cases, where QTL had anti-correlated effects on average petal number and trichome number; this detailed analysis revealed correlated changes in the effects during specific periods of development. For example, at *P-T11* the Ox allele increased trichome number for moving averages in flowers 1–17, after which it was no longer significant, while it was not significant for petal number until flower 11, after which it reduced petal number with increasing strength (Fig. 5c). The correlated change in the effect of the Ox allele leading to a reduction in both petal number and trichome number can be observed from approximately flower 10 onwards (Fig. 5c). In this light, *P-T11* acts similarly to *P-T1* although here, the Ox allele reduced both petal number and trichome number from flower 1 onwards, and later the magnitude of these effects reduced in concert (Fig. 5d). We found similar age-dependent effects for *P-T2* yet with a negative correlation in the change of both traits (Fig. 5e). Here, the Ox allele reduced trichome number until flower 15 with no significant effect on petal number, and it reduced petal number between flowers 16 and 24 with no significant effect on trichome number (Fig. 5e). We also observed age-dependent effects that were more temporally restricted for trichome number (*P-T10* and *12*) or petal number (*P-T3*, *19*). In fact, we found that *P-T8* and *9* had effects on petal number in a very restricted window spanning four flowers (two adjacent moving averages) that were not detectable in bins of five flowers (Fig. 4e). Taken together, these results suggest that allelic variation in general age-dependent mechanisms, trait-specific integrators of ageing signals, as well as genes specific to petal or sepal trichome number underlie these QTL.

Discussion

Variable petal number is derived in *C. hirsuta* from a stable petal number of four that characterizes the Brassicaceae. We found that petal number varied from zero to four within five *C. hirsuta* mapping populations and that this variation was highly heritable. We identified at least 15 loci with effects on average petal number that diverged between the six *C. hirsuta* accessions analysed here. Understanding this genetic architecture can provide insight into the genetic basis and evolutionary forces responsible for petal number variation in *C. hirsuta*. A polygenic architecture of many small to moderate effect QTL, affecting the trait in both positive and negative directions, likely contributes to maintaining *C. hirsuta* petal number within its variable range below four. In contrast to this, traits governed by large effect mutations with

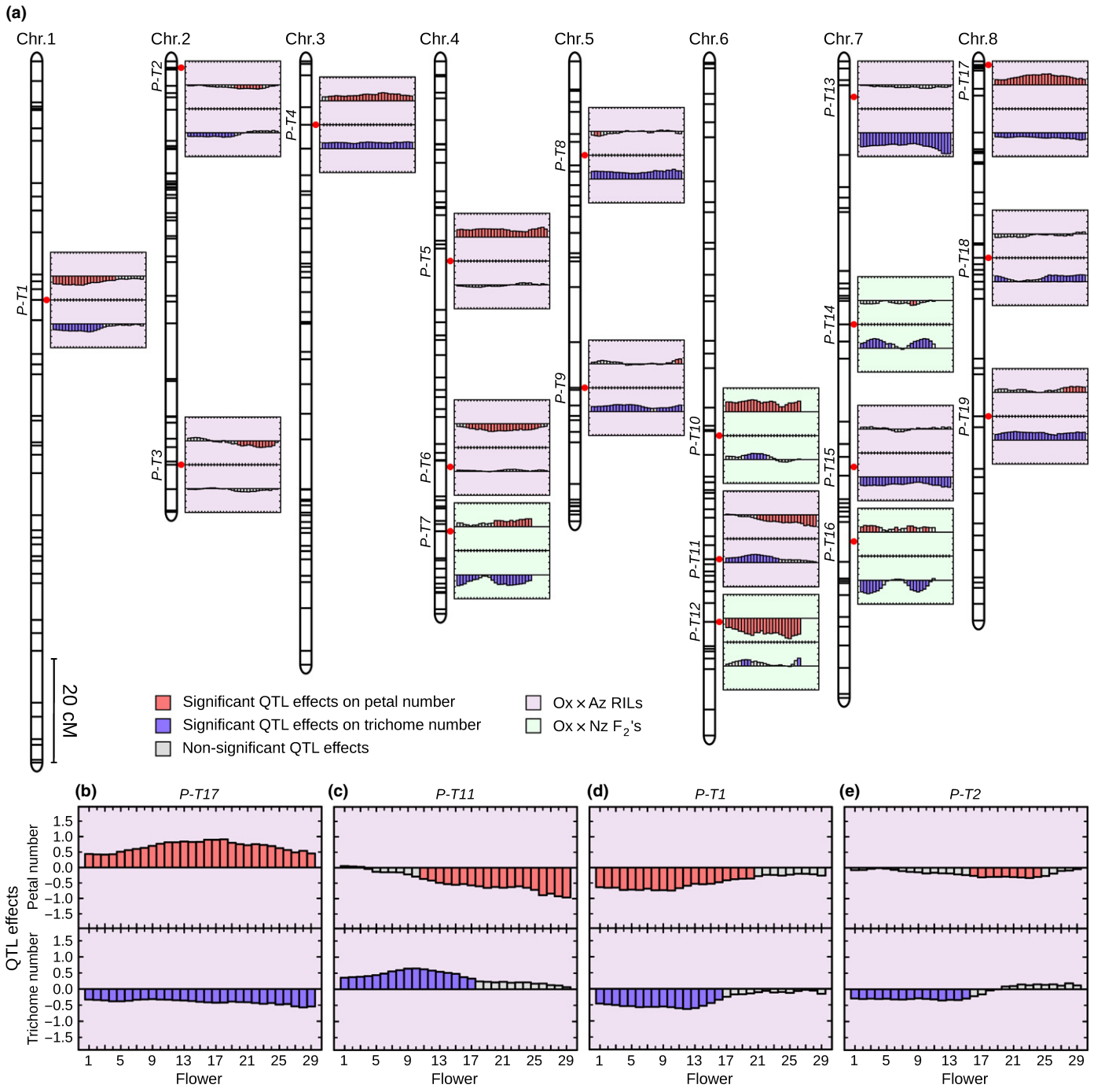

Fig. 5 Age-dependent effects of petal and sepal trichome number quantitative trait loci (QTL) in *Cardamine hirsuta*. (a) Allelic effects of QTL detected in the Ox × Az recombinant inbred lines (RILs) (pink background) and the Ox × Nz F_2 (green background) for petal and sepal trichome number in consecutive bins of five flowers (Fig. 4) on moving averages of these traits. Effects are shown plotted to the right of the linkage groups of the integrated genetic map. The position of each QTL is indicated by a red dot and QTL effects are plotted in the adjacent bar graphs. Significant effects on petal number are shown in red and on sepal trichome number in blue. Nonsignificant effects are shown in grey. Axis labels and numbering are omitted but are identical to those in (b). Note that the bi-modal distribution of QTL effects on trichome number for *P-T7*, *14* and *16* probably reflects the lack of phenotypic variation in flowers with no sepal trichomes that are produced at the mid-point of this age progression. (b–e) Detailed view of the allelic effects of four QTL.

low pleiotropy can respond to directional selection more readily, and under this type of architecture, the average petal number could readily revert back to four petals in *C. hirsuta*. We analysed an EMS mutant in *C. hirsuta* that increased the average petal number by two petals over the wild-type Ox value, without apparent pleiotropic effects. This phenotype of the *fp2* mutant demonstrates that *C. hirsuta* petal development could, in principle, accommodate natural allelic effects of this magnitude that would increase the average petal number and reduce phenotypic variability without incurring obvious pleiotropic effects on

development. Therefore, our results suggest that species-specific developmental constraints do not prevent *C. hirsuta* from attaining a high average petal number, but rather that a polygenic architecture contributes to maintaining the variable petal number in *C. hirsuta*.

In Brassicaceae species with a stable petal number of four, such as *A. thaliana*, this phenotype is robust to natural genetic variation. In contrast to this, petal number varied from zero to four in *C. hirsuta* and we detected at least 15 QTL at which natural allelic variation affected petal number. Additionally, the average petal number varied between isogenic individuals of the Ox accession in response to environmental variation that was unintentionally introduced between different experiments. Thus, evolutionary change has produced a nonrobust phenotype in *C. hirsuta* where petal number is shifted outside of the buffered zone that produces four petals in other crucifers (Monniaux *et al.*, 2015). Although petal number varied between zero and four in *C. hirsuta* flowers, it never increased beyond four. This indicates that phenotypic variation in *C. hirsuta* petal number is one-sided with respect to the buffered trait value of four petals that exists in most crucifers. Two-sided phenotypic variation is good evidence for a loss of developmental robustness as this can more readily produce a wider phenotypic distribution with a similar mean (Felix & Barkoulas, 2012). Therefore, the evolutionary transition from invariant to variable petal number that occurred in the lineage leading to *C. hirsuta* may not reflect a complete loss of robustness in this developmental patterning system, but rather a shift outside of its buffered zone.

Petal number variation is a character that defines *C. hirsuta* and manifests at different scales: from between genetically distinct accessions to between the different flowers produced on a single plant. By quantifying phenotypic variation at each of these scales we identified a significant contribution of plant ageing to petal number variation. Moreover, we found that petal number shared a common genetic basis with a temporally correlated trait: sepal trichome number, but not with lateral stamen number, even though each lateral stamen and its two adjacent petals are thought to share developmental commonalities such as pre-patterning from a single field of DORNROSCHEN-LIKE transcription factor expression (Chandler *et al.*, 2011). By considering both age-dependent traits simultaneously in a multi-trait QTL analysis of two mapping populations, we recovered a genetic architecture that was comparable to our single trait analysis of five mapping populations. Therefore, the increased power to detect QTL for correlated traits by multi-trait analysis allowed us to recover a similar genetic architecture in a less genetically diverse sample. Essentially, we used different rulers to measure the genetic basis of petal number as an age-dependent trait in our single and multi-trait approaches: either multiple mapping populations or multiple traits. We can illustrate this point with two QTL detected on chromosome 5: *P-T8* and *P-T9*. Alleles for these QTL in the Wa and Jpa1 accessions affected the average petal number and were detected in single trait analysis of five mapping populations that included these accessions. By contrast, alleles for these QTL in the Az accession affected the average trichome number and were detected in multi-trait analysis of two mapping populations that included this accession. In fact, we found that while the sepal trichome number was affected in all flowers we could also identify a specific temporal window where these alleles affected petal number. Therefore, recognizing that petal number varied across scales and accurately accounting for this in our analysis by (1) phenotyping in an age-dependent manner and (2) conducting multi-trait QTL analysis with a temporally correlated trait, increased our power to resolve QTL locations and to detect allelic effects. Moreover, by determining that a common genetic basis governed petal number and sepal trichome number we could take advantage of the greater phenotypic range observed in sepal trichomes.

Using *C. hirsuta*, we have characterized the genetic basis of the phenotypic variation expressed in the normally invariant trait of petal number. This raises questions about the origin of this genetic variation. The accumulation of variation in a background that suppresses its expression has been recognized for its potential contribution to evolutionary processes (Masel, 2006). Cryptic variation has been shown to play a role in the evolution of eye loss in Mexican cave fish where rapid adaptation to a new environment can occur via the release of standing variation for eye size, which was phenotypically masked by HSP90 (Rohner *et al.*, 2013). There is also evidence that a truly robust phenotype like vulva cell fate patterning in *Caenorhabditis* evolves by accumulating cryptic variation (Felix, 2007; Milloz *et al.*, 2008). We found that petal number variation in *C. hirsuta* has a genetic architecture of many small to moderate effect QTL. These loci comprise genetic variation that is available in *C. hirsuta* to alter petal number and for a considerable number of them also sepal trichome number. The distribution of sepal trichomes shows natural variation in both *C. hirsuta* and *A. thaliana* (Shikata *et al.*, 2009), whereas petal number varies only in *C. hirsuta*. Therefore, genetic variation with the potential to influence petal number may exist in *A. thaliana* and other closely related species with a robust number of petals, but this variation remains cryptic for petals. Studying the genetic architecture of petal number in *C. hirsuta*, therefore, provides a comparative framework to test this hypothesis in *A. thaliana*. Identifying the genes underlying the QTL detected here will also help us to understand which components of the gene regulatory network underlying petal development were targeted during evolution to generate phenotypic variation.

Studying the genetic architecture of petal number variation also provides some insights into the evolutionary significance of this trait. We have shown that many of the loci responsible for variation in petal number also affect sepal trichome number and there might be more pleiotropic effects on other age-dependent traits. Furthermore, the age-dependent effects of some petal number QTL indicate that the underlying genes may be involved in temporal processes that are potentially important for many plant functions. Therefore, it is possible that selection on these pleiotropic traits contributes to maintaining petal number within its variable range. An alternative hypothesis is that the ability to vary petal number, particularly in response to the environment, is an adaptive trait in *C. hirsuta*. Petal reduction is a characteristic of dimorphic cleistogamy: the ability to produce both outcrossing

flowers with petals (chasmogamous) and obligatory self-pollinating flowers with reduced or absent petals (cleistogamous) (Culley & Klooster, 2007). As a selfing species, *C. hirsuta* seems to efficiently self-pollinate under standard glasshouse conditions irrespective of petal number variation, but these conditions hardly reflect the real world. Therefore, it will be interesting to address whether variable petal number contributes to the life history strategy of *C. hirsuta* as an invasive, pioneer weed with a cosmopolitan distribution (Hay *et al.*, 2014).

Acknowledgements

We thank M. Tsiantis, and members of his group (A. Tattersall, M. Cartolano, J. Lamb and S. Langer) for generating and making available the *C. hirsuta* RIL populations and providing sequence and molecular marker information. We thank M. Tsiantis for critical comments on the manuscript, M. Bonsall for helpful discussions and S. McKim for a scanning electron micrograph. This work was supported by Biotechnology and Biological Sciences Research Council grant BB/H01313X/1 to A.H. and A.H. was supported by the Max Planck Society W2 Minerva programme and a Royal Society University Research Fellowship and M.M. by a European Molecular Biology Organization Long Term Fellowship.

References

Benkova E, Michniewicz M, Sauer M, Teichmann T, Seifertova D, Jurgens G, Friml J. 2003. Local, efflux-dependent auxin gradients as a common module for plant organ formation. *Cell* **115**: 591–602.

Bowman JL, Smyth DR, Meyerowitz EM. 1991. Genetic interactions among floral homeotic genes of Arabidopsis. *Development* **112**: 1–20.

Brewer PB, Howles PA, Dorian K, Griffith ME, Ishida T, Kaplan-Levy RN, Kilinc A, Smyth DR. 2004. *PETAL LOSS*, a trihelix transcription factor gene, regulates perianth architecture in the *Arabidopsis* flower. *Development* **131**: 4035–4045.

Cartolano M, Pieper B, Lempe J, Tattersall A, Huijser P, Tresch A, Darrah PR, Hay A, Tsiantis M. 2015. Heterochrony underpins natural variation in *Cardamine hirsuta* leaf form. *PNAS*. doi: 10.1073/pnas.1419791112.

Chandler JW, Jacobs B, Cole M, Comelli P, Werr W. 2011. *DORNROSCHEN-LIKE* expression marks *Arabidopsis* floral organ founder cells and precedes auxin response maxima. *Plant Molecular Biology* **76**: 171–185.

Coen ES, Meyerowitz EM. 1991. The war of the whorls: genetic interactions controlling flower development. *Nature* **353**: 31–37.

Culley TM, Klooster MR. 2007. The Cleistogamous breeding system: a review of its frequency, evolution, and ecology in angiosperms. *Botanical Review* **73**: 1–30.

Doebley J, Stec A, Hubard L. 1997. The evolution of apical dominance in maize. *Nature* **386**: 485–488.

Eshed Y, Baum SF, Perea JV, Bowman JL. 2001. Establishment of polarity in lateral organs of plants. *Current Biology* **11**: 1251–1260.

Felix MA. 2007. Cryptic quantitative evolution of the vulva intercellular signaling network in Caenorhabditis. *Current Biology* **17**: 103–114.

Felix MA, Barkoulas M. 2012. Robustness and flexibility in nematode vulva development. *Trends in Genetics* **28**: 185–195.

Fisher RA. 1918. The correlation between relatives on the supposition of mendelian inheritance. *Transactions of the Royal Society of Edinburgh* **52**: 399–433.

Hay A, Tsiantis M. 2006. The genetic basis for differences in leaf form between *Arabidopsis thaliana* and its wild relative *Cardamine hirsuta*. *Nature Genetics* **38**: 942–947.

Hay AS, Pieper B, Cooke E, Mandakova T, Cartolano M, Tattersall AD, Ioio RD, McGowan SJ, Barkoulas M, Galinha C *et al.* 2014. *Cardamine hirsuta*: a versatile genetic system for comparative studies. *Plant Journal* **78**: 1–15.

Huang T, Lopez-Giraldez F, Townsend JP, Irish VF. 2012. RBE controls microRNA164 expression to effect floral organogenesis. *Development* **139**: 2161–2169.

Irish VF. 2008. The Arabidopsis petal: a model for plant organogenesis. *Trends in Plant Science* **13**: 430–436.

Johanson U, West J, Lister C, Michaels S, Amasino R, Dean C. 2000. Molecular analysis of FRIGIDA, a major determinant of natural variation in Arabidopsis flowering time. *Science* **290**: 344–347.

Johnston SE, Gratten J, Berenos C, Pilkington JG, Clutton-Brock TH, Pemberton JM, Slate J. 2013. Life history trade-offs at a single locus maintain sexually selected genetic variation. *Nature* **502**: 93–95.

Krizek BA, Lewis MW, Fletcher JC. 2006. *RABBIT EARS* is a second-whorl repressor of *AGAMOUS* that maintains spatial boundaries in Arabidopsis flowers. *Plant Journal* **45**: 369–383.

Lampugnani ER, Kilinc A, Smyth DR. 2012. *PETAL LOSS* is a boundary gene that inhibits growth between developing sepals in *Arabidopsis thaliana*. *Plant Journal* **71**: 724–735.

Lampugnani ER, Kilinc A, Smyth DR. 2013. Auxin controls petal initiation in Arabidopsis. *Development* **140**: 185–194.

Manolio TA, Collins FS, Cox NJ, Goldstein DB, Hindorff LA, Hunter DJ, McCarthy MI, Ramos EM, Cardon LR, Chakravarti A *et al.* 2009. Finding the missing heritability of complex diseases. *Nature* **461**: 747–753.

Masel J. 2006. Cryptic genetic variation is enriched for potential adaptations. *Genetics* **172**: 1985–1991.

Michaels SD, Amasino RM. 1999. *FLOWERING LOCUS C* encodes a novel MADS domain protein that acts as a repressor of flowering. *Plant Cell* **11**: 949–956.

Milloz J, Duveau F, Nuez I, Felix MA. 2008. Intraspecific evolution of the intercellular signaling network underlying a robust developmental system. *Genes & Development* **22**: 3064–3075.

Monniaux M, Pieper B, Hay A. 2015. Stochastic variation in *Cardamine hirsuta* petal number. *Annals of Botany*, in press. doi: 10.1093/aob/mcv131.

Orr HA. 1998. Testing natural selection vs. genetic drift in phenotypic evolution using quantitative trait locus data. *Genetics* **149**: 2099–2104.

Rockman MV. 2012. The QTN program and the alleles that matter for evolution: all that's gold does not glitter. *Evolution* **66**: 1–17.

Rohner N, Jarosz DF, Kowalko JE, Yoshizawa M, Jeffery WR, Borowsky RL, Lindquist S, Tabin CJ. 2013. Cryptic variation in morphological evolution: HSP90 as a capacitor for loss of eyes in cavefish. *Science* **342**: 1372–1375.

Shapiro MD, Marks ME, Peichel CL, Blackman BK, Nereng KS, Jonsson B, Schluter D, Kingsley DM. 2004. Genetic and developmental basis of evolutionary pelvic reduction in threespine sticklebacks. *Nature* **428**: 717–723.

Shikata M, Koyama T, Mitsuda N, Ohme-Takagi M. 2009. Arabidopsis SBP-box genes *SPL10, SPL11* and *SPL2* control morphological change in association with shoot maturation in the reproductive phase. *Plant and Cell Physiology* **50**: 2133–2145.

Specht CD, Bartlett ME. 2009. Flower evolution: the origin and subsequent diversification of the angiosperm flower. *Annual Review of Ecology Evolution and Systematics* **40**: 217–243.

Stern DL, Orgogozo V. 2008. The loci of evolution: how predictable is genetic evolution? *Evolution* **62**: 2155–2177.

Takeda S, Matsumoto N, Okada K. 2004. *RABBIT EARS*, encoding a SUPERMAN-like zinc finger protein, regulates petal development in *Arabidopsis thaliana*. *Development* **131**: 425–434.

Telfer A, Bollman KM, Poethig RS. 1997. Phase change and the regulation of trichome distribution in *Arabidopsis thaliana*. *Development* **124**: 645–654.

Van Ooijen JW 2006. *Joinmap® 4, software for the calculation of genetic linkage maps in experimental populations*. Wageningen, the Netherlands: Kyazma B.V.

VSN International. 2013. *GenStat for Windows, 16th edn*. Hemel Hempstead, UK: VSN International.

Wang J-W, Czech B, Weigel D. 2009. miR156-regulated SPL transcription factors define an endogenous flowering pathway in *Arabidopsis thaliana*. *Cell* **138**: 738–749.

Yu N, Cai WJ, Wang S, Shan CM, Wang LJ, Chen XY. 2010. Temporal control of trichome distribution by microRNA156-targeted *SPL* genes in *Arabidopsis thaliana*. *Plant Cell* **22**: 2322–2335.

Supporting Information

Additional supporting information may be found in the online version of this article.

Fig. S1 An integrated genetic map for the five experimental *C. hirsuta* populations analysed.

Fig. S2 Genome-wide QTL mapping scans for average petal number in five *C. hirsuta* populations.

Fig. S3 Genome-wide multi-trait QTL mapping scans for average petal number and average trichome number in two *C. hirsuta* populations.

Fig. S4 Genome-wide multi-trait QTL mapping scans for petal number and trichome number averaged in bins of five flowers in two *C. hirsuta* populations.

Table S1 Phenotypic variances explained for average petal number by the full QTL models in five mapping populations

Table S2 Positions of multi-trait QTL detected for petal number and sepal trichome number averaged in nonoverlapping bins of five flowers

Table S3 Effects of multi-trait QTL detected for petal number and sepal trichome number averaged in nonoverlapping bins of five flowers in the Ox × Az RIL population

Table S4 Effects of multi-trait QTL detected for petal number and sepal trichome number averaged in nonoverlapping bins of five flowers in the Ox × Nz F_2 population

Table S5 Effects of multi-trait QTL detected for petal number and sepal trichome number averaged in nonoverlapping bins of five flowers in the Ox × Az RIL population on moving averages

Table S6 Effects of multi-trait QTL detected for petal number and sepal trichome number averaged in nonoverlapping bins of five flowers in the Ox × Nz F_2 population on moving averages

Please note: Wiley Blackwell are not responsible for the content or functionality of any supporting information supplied by the authors. Any queries (other than missing material) should be directed to the *New Phytologist* Central Office.